*- Technical Paper -*

# NON-DESTRUCTIVE TEST OF HEATED FIBER REINFORCED HIGH STRENGTH CONCRETE

Sofren L. SUHAENDI[*1], Kazunori SHIMURA[*2], and Takashi HORIGUCHI[*3]

ABSTRACT

A catastrophic failure mechanism termed as explosive spalling might be observed on high strength concrete (HSC) exposed to high temperature condition. Fortunately, mitigation of this type of failure mechanism could be achieved by the addition of polypropylene fiber inside concrete mixture. Nevertheless, further usage possibility of concrete structure surviving fire accident will depend on its residual properties. This paper presents correlation between ultrasonic pulse velocity (UPV) test and residual properties of fiber reinforced HSC in the aftermath of heat exposition.

Keywords: high strength concrete, fire resistance, residual properties, non-destructive test

## 1. INTRODUCTION

High strength concrete (HSC) is commonly produced by the reduction of water to cement ratio (W/C) of concrete mix proportion. Other ways include the addition and/or replacement of cement by mineral admixtures such as fly ash, silica fume, and ground granulated blast furnace slag. Hydration of these cementitious materials will create matrix networks with extremely low void structure, improving its mechanical and permeability performance. With the soaring usage of HSC at the construction sites, better understanding on this type of concrete has become an inevitable necessity.

In spite of its superior performance, high strength concrete HSC was prone to catastrophic failure mechanism, termed as explosive spalling, under elevated temperature condition [1]. Some papers reported that this type of failure mechanism was closely related to the low permeability property of HSC. During exposition to high temperature, denser matrix of HSC would prevent water vapor escaping quickly. As temperature increased, this water vapor was accumulated inside the concrete matrix and build-up of a significant pore pressure was generated. Once the accumulation of pore pressure exceeds HSC tensile strength, it would spall in an explosive manner.

Other possible factor causing explosive spalling of HSC exposed to high temperature was thermal incompatibility between coarse aggregate and hardened cement paste (hcp). During exposition to high temperature, coarse aggregate would tend to expand while hcp would tend to shrink. This incompatibility would induce build-up of strain energy that might play a secondary role in explosive spalling mechanism [2]. HSC containing siliceous aggregate inside its mixture was reported to be more prone to explosive spalling compared with the one using calcareous aggregate. Until now, true mechanism of explosive spalling of HSC exposed to high temperature was not well defined.

Recent development in mitigating explosive spalling failure mechanism was achieved by the addition of organic fibers, such as polypropylene fibers, into HSC mixture [3, 4]. The melting of this type of fibers would create passages for the reduction of pore pressure inside the concrete matrix when HSC was exposed to high temperature. Unfortunately, as the consequence of generated additional pores inside the concrete matrix, residual properties of concrete surviving high temperature exposition would decrease significantly [5]. Therefore, it would be of great importance to investigate the deterioration of the surviving concrete as further necessary adjustment to the structure would depend on the residual

*1 Graduate Student, Dept. of Civil Engineering, Hokkaido University, M.E., JCI Member
*2 Research Associate, Dept. of Civil Engineering, Hokkaido University, Dr.E., JCI Member
*3 Associate Prof., Dept. of Civil Engineering, Hokkaido University, Dr.E., JCI Member

properties.

In non-destructive test measurement field, ultrasonic pulse velocity test (UPV) is well-known for its practicality allowing quick and reliable measurement of internal flaws inside the material without cutting or sectioning a part [6]. In this experimental study, UPV test was performed as to establish a correlation between velocity and properties of concrete, before and in the aftermath of exposition to high temperature.

## 2. EXPERIMENT

### 2.1 Materials

(1) Short fibers

Polypropylene and steel fibers having 60 and 600 micron effective diameter were used in this experimental study. Both polypropylene and steel fibers came in bundles that were well dispersed inside the concrete mixture Properties of short fibers are shown in Table 1.

Table 1 Properties of short fibers

| | Polypropylene | | Steel |
|---|---|---|---|
| Diameter (mm) | 0.06 | | 0.6 |
| Length (mm) | 6 | 30 | 30 |
| Shape | Fibrillated | | Straight-hooked |
| Density (gr/cm$^3$) | 0.9 | | 7.8 |
| $T_{melt}$ ($^oC$) | 160-170 | | 1370 |
| $T_{vaporize}$ ($^oC$) | 341 | | – |

(2) Concrete specimens

All series of concrete mixture were cast using ordinary portland cement, river sand, and river gravel. Fineness modulus of river sand was 2.9 and maximum nominal size of river gravel was 20 mm. Some mixing design parameters were kept constant: W/C of 0.3, sand to aggregate ratio (s/a) of 60%, and water content of 170 kg/m$^3$. A polycarboxylate-based superplasticizer, air entraining, and bubble cutter agent were used to attain desired workability (slump flow of 400-600 mm) and air content (5-7%) of fresh concrete.

Concrete cylinders of 100-mm diameter size were cast and cured under lime-saturated water at temperature of 20±2 $^oC$ for 28 days. Then, some specimens were heated using electric furnace. Heating rate was set at 10 $^oC$ per minute with maximum temperature kept at 200 and 400 $^oC$ for two hours. Preventing thermal cracking upon cooling, heated specimens were let to cool inside the furnace until its temperature coincided with room temperature.

Table 2 Mixture proportion

| Series | Fiber vol. (%) | | SP | AE | BC |
|---|---|---|---|---|---|
| | PP | Steel | (%×c) | (A) | (T) |
| Plain | - | - | 1.3 | 7 | - |
| P6-0.25 | 0.25 | - | 1.3 | 3 | 1 |
| P6-0.5 | 0.5 | - | 1.3 | 3 | 1 |
| P30-0.25 | 0.25 | - | 1.7 | 3 | 2 |
| P30-0.5 | 0.5 | - | 1.9 | 3 | 2 |
| S30-0.25 | - | 0.25 | 1.3 | 3 | 1 |
| S30-0.5 | - | 0.5 | 1.3 | 3 | 1 |
| HY1$^\dagger$ | 0.25 | 0.5 | 1.3 | 1 | 4 |
| HY2$^\dagger$ | 0.5 | 0.25 | 1.4 | 1 | 4 |

1A= 0.004%×cement (by mass)

1T= 0.0002%×cement (by mass)

$^\dagger$both HY1 and HY2 use 6-mm long PP fibers

### 2.2 Experimental Method

(1) Loading and non-destructive test

Compressive and splitting tensile strength test for heated and non-heated specimens were performed according to JIS A1108 and A1113. Loading rate was set at 250 kPa/s and 25 kPa/s for compressive and tensile strength tests respectively. A commercial non-destructive test measurement, PUNDIT, was adopted to measure ultrasonic pulse velocity of concrete specimens. Readings were performed in longitudinal direction applying frequency of 200 kHz.

(2) Permeability test

Specimens were set inside the permeability cell test apparatus, shown in Fig. 1. Pressure was applied by means of nitrogen gas once the cell was filled with deaired water. Assuming water flow through concrete specimens to be continuous and laminar, water permeability coefficient was calculated based on Darcy's formula. Due to the nature of pore structure of concrete specimens (before and after heating), two methods of tests were performed.

Input method—A pressure of 1.5 MPa, representing approximately 150 meters of drop in hydraulic head, was applied for a few days. Water penetration depth was measured after breaking the specimen. Then several readings of penetration depth were performed along specimen height. Water permeability coefficient of specimen was calculated as follows:

$$k = \frac{d^2}{2ht} \qquad (1)$$

where,

$k$ : water permeability coefficient (m/s)

$d$ : water penetration depth (m)

$h$ : water head (m)

$t$ : time (s)

Output method—Reading of water outflow that permeated through concrete specimen was performed until steady state flow had been achieved. Water permeability coefficient of specimen was calculated as follows:

$$k = \frac{\rho Q}{2\pi HP} \ln \frac{r_o}{r_i} \tag{2}$$

where,

$\rho$ : water density (kg/m$^3$)
$Q$ : water outflow (m$^3$/s)
$H$ : specimen height (m)
$P$ : water pressure (kgf/m$^2$)
$r_o$ : specimen radius (m)
$r_i$ : central hole radius (m)

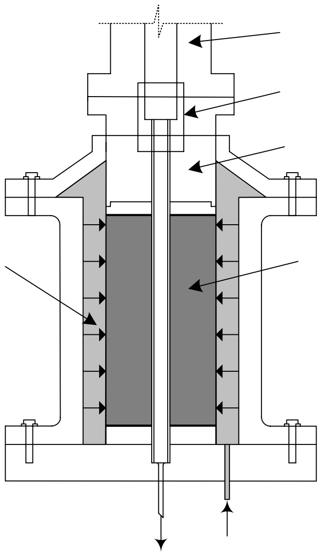

Fig. 1 Permeability cell

## 3. RESULTS AND DISCUSSIONS

### 3.1 Residual properties

Fig. 2 shows deterioration of concrete quality by means of UPV measurements. UPV reduces almost proportionally with the increase in maximum heating temperature. Generation of pores and cracks resulting from physicochemical changes and thermal incompatibility between aggregate and cement paste are believed to be responsible for the deterioration in heated concrete properties. Averaging UPV measurements data of all series, reduction of velocity from 4.6 to 2.8 km/s can be observed with the increase in temperature from 20 to 400 $^{o}$C.

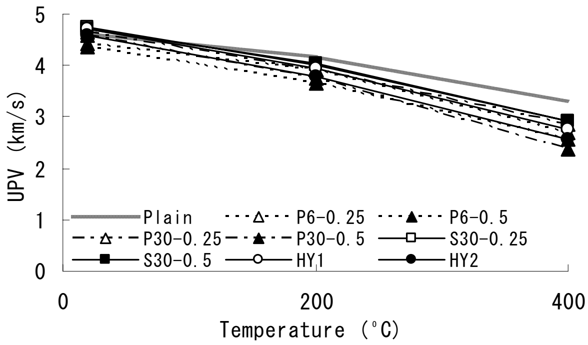


Fig. 2 Residual UPV measurements

Fig. 3-5 shows reduction of mechanical properties with the increase in maximum heating temperature. Compared with other mechanical properties being measured, modulus of elasticity shows a more rapid degradation. Average reduction of all series in compressive strength, tensile strength, and modulus of elasticity is 15, 23, and 27% after 200 $^{o}$C and 39, 43, and 67% after 400 $^{o}$C.

In relation to gradient steepness of relative residual properties shown in Fig. 5 and referring to residual properties shown in Table 4, steel fiber reinforced HSC (SFRHSC) is observed to be more effective in keeping its residual tensile properties compared with polypropylene fiber reinforced HSC (PFRHSC) and hybrid fiber reinforced HSC (HFRHSC). The main reason for this is due to the fact that SFRHSC did not suffer melting or vaporization of its fibers constituent. As polypropylene fibers melt at 160-170 $^{o}$C and vaporize at 341 $^{o}$C, HSC containing these fibers will tend to suffer more reduction in its properties after heating at 200 and 400 $^{o}$C. Nevertheless, in terms of explosive spalling mitigation mechanism, HSC containing polypropylene fibers shows better performance as melting of these fibers will create passages that allow reduction of pore pressure inside the concrete matrix.

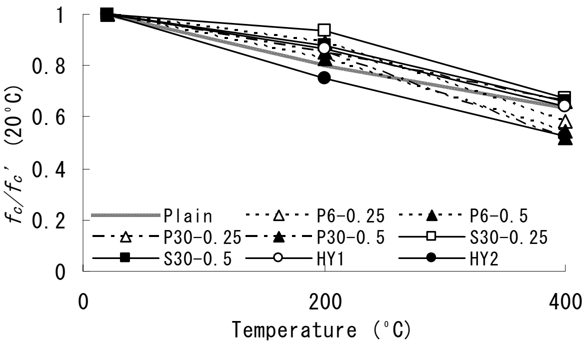


Fig. 3 Relative compressive strength

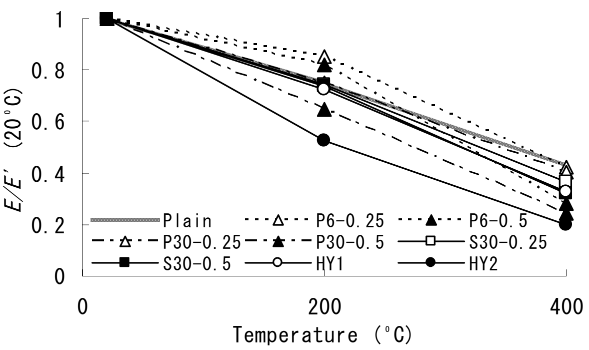


Fig. 4 Relative modulus of elasticity

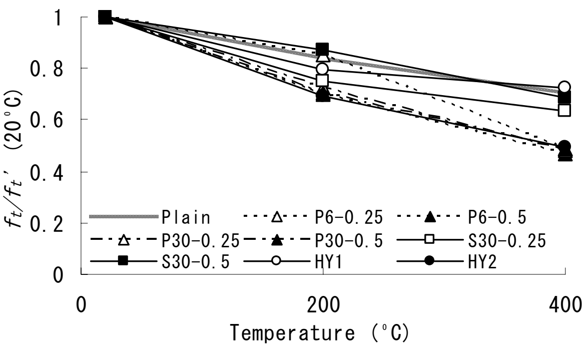


Fig. 5 Relative tensile strength

Reduction in mechanical properties of HSC containing polypropylene fibers will closely depend on fiber volume fraction ($V_f$) rather than fiber length ($l_f$). As shown in Table 3-5, more inclusion of these fibers inside concrete mixture will generate more pores thus deteriorating residual properties as a consequence. In Table 4, it is obviously shown that reduction in residual modulus of elasticity after 400 $^{o}$C for this type of concrete will depend closely on the amount of its fiber volume fraction. On the contrary, in the case of HSC containing steel fibers, more inclusion of these fibers will improve the residual tensile strength.

The basic idea of using hybrid fibers in this experimental study is to have a synergy between these two types of fibers. During HSC exposition to high temperature, polypropylene fibers will be expected to mitigate explosive spalling failure mechanism while steel fibers will maintain its properties afterwards. From data results of HFRHSC series, it is shown that HY2 residual properties degrade more rapidly compared with HY1. Regardless of both series having the same total fiber volume fraction ($V_f$ = 0.75%), HY1 contains half volume of polypropylene fibers and twice volume of steel fibers than those of HY2. Thus, it is obvious that proportioning of hybrid fibers at mix design stage will control the behavior of HFRHSC during and after heat exposition.

Fig. 6 shows increase in water permeability coefficient with the increase in maximum heating temperature. Compared with other series, plain HSC shows the lowest rate of increase in water permeability coefficient. This result may confirm HSC vulnerability to explosive spalling during exposition to high temperature as it has low permeability that prevents vapor pressure to escape. After heating at 400 $^{o}$C, water permeability coefficient of HSC only increase to 17 times of its original value, comparing to other series that can reach an increase of 3 orders of magnitude.

In terms of PFRHSC series, residual water permeability coefficient is closely related to both $V_f$ and $l_f$. More fiber inclusion will increase the permeability coefficient as it generates more pores while longer fiber will interconnect the pores hence providing pathway for water permeation. With more polypropylene fibers inside HY2 mixture, its water permeability coefficient also increase more compared with HY1.

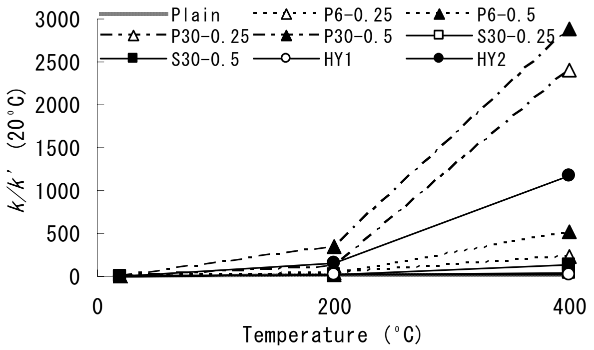


Fig. 6 Relative permeability coefficient

## 3.2. Correlation

Table 3-5 shows test data obtained from this experimental study. Correlation between these data would be presented onward.

Table 3 Residual UPV and $f_c'$

| Series | Ultrasonic pulse velocity (km/s) | | | Compressive strength (MPa) | | |
|---|---|---|---|---|---|---|
| | 20 | 200 | 400 | 20 | 200 | 400 |
| Plain | 4.62 | 4.15 | 3.29 | 81.6 | 65.2 | 51.8 |
| P6-0.25 | 4.42 | 3.91 | 2.68 | 60.8 | 54.1 | 35.6 |
| P6-0.5 | 4.36 | 3.66 | 2.57 | 60.0 | 49.8 | 32.7 |
| P30-0.25 | 4.65 | 3.90 | 2.85 | 71.9 | 61.3 | 47.4 |
| P30-0.5 | 4.58 | 3.74 | 2.37 | 59.4 | 50.7 | 30.9 |
| S30-0.25 | 4.73 | 3.99 | 2.93 | 68.0 | 63.6 | 45.8 |
| S30-0.5 | 4.71 | 4.03 | 2.92 | 75.1 | 66.1 | 49.8 |
| HY1 | 4.70 | 3.94 | 2.74 | 59.7 | 51.6 | 38.3 |
| HY2 | 4.60 | 3.79 | 2.57 | 65.5 | 49.2 | 34.3 |

Table 4 Residual $E$ and $f_t'$

| Series | Modulus of elasticity (GPa) | | | Tensile strength (MPa) | | |
|---|---|---|---|---|---|---|
| | 20 | 200 | 400 | 20 | 200 | 400 |
| Plain | 34.2 | 25.8 | 14.8 | 4.4 | 3.7 | 3.1 |
| P6-0.25 | 32.4 | 27.7 | 13.8 | 4.1 | 3.5 | 2.0 |
| P6-0.5 | 29.6 | 24.3 | 8.3 | 4.3 | 3.0 | 2.0 |
| P30-0.25 | 33.2 | 24.9 | 13.4 | 5.4 | 3.9 | 2.6 |
| P30-0.5 | 32.4 | 20.9 | 7.9 | 4.7 | 3.3 | 2.3 |
| S30-0.25 | 36.8 | 27.3 | 13.6 | 5.2 | 3.9 | 3.3 |
| S30-0.5 | 41.7 | 30.6 | 13.3 | 5.4 | 4.7 | 3.7 |
| HY1 | 34.9 | 25.3 | 11.5 | 5.4 | 4.3 | 3.9 |
| HY2 | 45.8 | 24.2 | 9.0 | 5.5 | 3.8 | 2.7 |

Table 5 Residual $k$

| Series | Permeability coefficient ($\times 10^{-12}$ m/s) | | |
|---|---|---|---|
| | 20 | 200 | 400 |
| Plain | 2.4 | 47 | 44 |
| P6-0.25 | 3.8 | 175 | 884 |
| P6-0.5 | 15.5 | 394 | 8130 |
| P30-0.25 | 14.0 | 1660 | 33700 |
| P30-0.5 | 17.9 | 6180 | 51500 |
| S30-0.25 | 22.2 | 528 | 945 |
| S30-0.5 | 5.2 | 115 | 728 |
| HY1 | 68.1 | 852 | 1870 |
| HY2 | 5.7 | 852 | 6640 |

Fig. 7-10 shows correlations between velocity and properties of HSC after and before exposition to high temperature. In this experimental study, velocity of 3.3 and 4.2 km/s marks the clustering of data. Specimens heated at 400 °C will correspond to velocity less than 3.3 km/s while the non-heated ones will correspond to velocity of more than 4.2 km/s. Meanwhile, specimens heated at 200 °C will lie between 3.3-4.2 km/s.

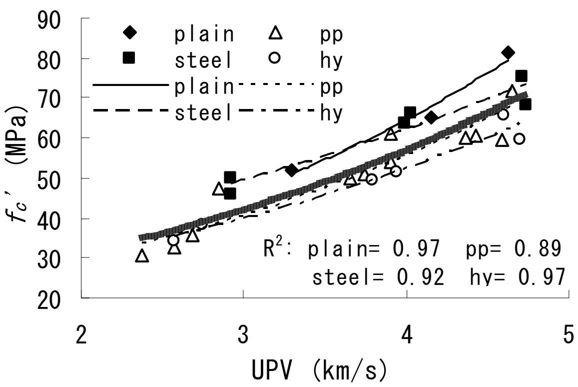


Fig. 7 Compressive strength—UPV

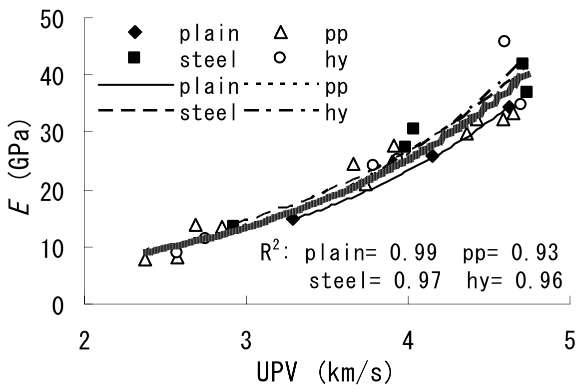


Fig. 8 Modulus of elasticity—UPV

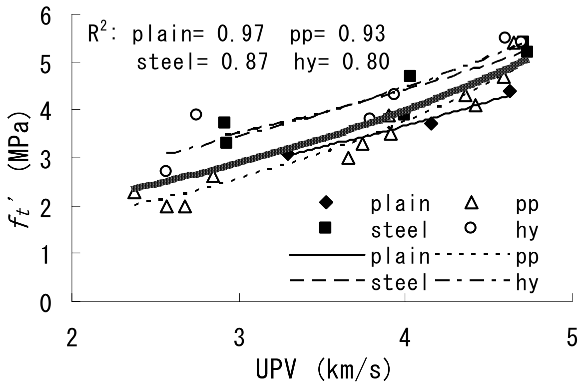


Fig. 9 Tensile strength—UPV

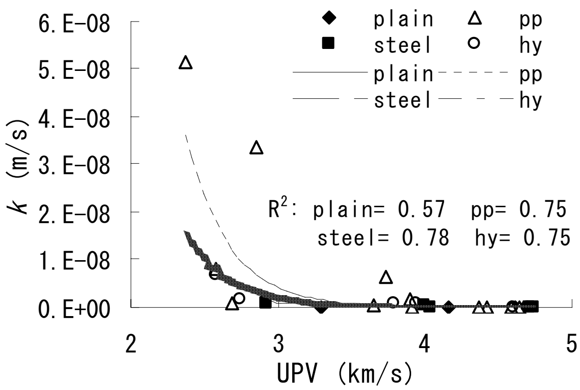


Fig. 10 Permeability coefficient—UPV

To analyze the correlation between velocity and properties of HSC before and after heating, regression analysis was performed. The thickest line inside the figures represents regression analysis including all data series while thinner ones represent regression analysis of some particular series (plain, PFRHSC, SFRHSC and HFRHSC). Exponential equations of regression analysis incorporating all data are given in Eq. (3)-(6). In the case of regression analysis of some particular series, correlation coefficient ($R^2$) is given for each particular series inside the figures.

$$f_c = 17.244e^{0.30v} \quad (3)$$

$$E = 2.0503e^{0.63v} \quad (4)$$

$$f_t = 1.1054e^{0.32v} \quad (5)$$

$$k = 2 \times 10^{-5} e^{-2.99v} \quad (6)$$

where,
$f_c$= compressive strength (MPa)
$E$= modulus of elasticity (GPa)
$f_t$= tensile strength (MPa)
$k$= water permeability coefficient (m/s)
$v$= ultrasonic pulse velocity (km/s)

Correlation coefficient ($R^2$) between velocity and compressive strength, modulus of elasticity, tensile strength, and water permeability coefficient of all data series are 0.84, 0.94, 0.76, and 0.7, respectively. From the analysis, it is shown that UPV test may have the possibility to be utilized to predict the properties of HSC before and after the exposition of high temperature. However, more experimental study to establish a more reliable correlation should be done before it should be used in practice allowing inspection of fire damaged concrete quicker and more efficient.

## 5. CONCLUSIONS

(1) High strength concrete quality degrades with the increase in maximum heating temperature as shown in UPV measurements. Reduction in velocity from 4.6 to 2.8 km/s may be observed with the increase in temperature from 20 to 400 $^{o}$C.

(2) More inclusion of polypropylene fibers inside HSC mixture will degrade its residual properties due to melting of these fibers. On the other hand, inclusion of more steel fibers will tend to improve residual tensile strength of heated HSC.

(3) In terms of HFRHSC, degradation trend of this type of concrete after heat exposition will depend on proportion of hybrid fibers added inside the mixture. More addition of polypropylene fibers will tend to reduce its residual properties.

(4) Water permeability coefficient of heated PFRHSC is quite sensitive to length of polypropylene fibers added into the concrete mixture. Longer fibers will interconnect the pores after melting thus allowing water to permeate easily through the concrete.

(5) Correlations between UPV and residual properties of FRHSC may become a useful tool allowing inspection of fire damaged concrete to be quicker and more efficient.

## REFERENCES


[1] Castillo, C. and Durrani, A.J., “Effect of Transient High Temperature on High-Strength Concrete”, ACI Materials Journal, Vol. 87, Jan. 1990, pp. 47-53

[2] Phan, L.T., Lawson, J.R., Davis, F.L., ”Effects of Elevated Temperature Exposure on Heating Characteristics, Spalling, and Residual Properties of High Performance Concrete,” Materials and Structures, Vol. 34, Mar. 2001, pp 83-91

[3] Bilodeau, A., Malhotra, V.M., and Hoff, G.C., “Hydrocarbon Fire Resistance of High Strength Normal Weight and Light Weight Concrete Incorporating Polypropylene Fibers,” Internasional Symposium on High Performance and Reactive Powder Concretes, 1998, pp. 271-296

[4] Shuttleworth, P., “Fire Protection of Concrete Tunnel Linings,” Proceedings of the Third International Conference on Tunnel Fires, Oct. 2001, pp. 157-165

[5] Suhaendi, S.L., Horiguchi T., and Saeki, N., “Permeability of Heated Fiber Reinforced High Strength Concrete,” Proceedings of the JCI, Vol. 26, Jul. 2004, pp. 315-320

[6] Popovics, S., “Analysis of the Concrete Strength versus Ultrasonic Pulse Velocity Rzelationship,” Material Evaluation, Vol. 59, Feb. 2001, pp. 123-129

[7] Horiguchi, T. and Sakai, K., “Hybrid Effects of Fiber-Reinforced Concrete on Fracture Toughness,” ACI SP-172, 1997, pp. 535-548

[8] Horiguchi, T., Sugawara T., and Saeki, N., “Fire Resistance of Hybrid Fiber Reinforced Concrete, 6th RILEM Symposium on FRC, 2004, pp. 669-678

[9] Janotka, I. and Bágel, L., “Pore Structures, Permeabilities, and Compressive Strengths of Concrete at Temperatures up to 800°C,” ACI Materials Journal, Vol. 99, Feb. 2002, pp. 196-200

[10] Bayasi, Z. and Al Dhaheri, M., “Effect of Exposure to Elevated Temperature on Polypropylene Fiber-Reinforced Concrete,” ACI Materials Journal, Vol. 99, Jan. 2002, pp. 22-26

[11] Sullivan, P.J.E., “A Probabilistic Method of Testing for the Assessment of Deterioration and Explosive Spalling of High Strength Concrete Beams in Flexure at High Temperature, Cement and Concrete Composite Journal, Vol. 26, 2004, pp. 155-162